Trends in Analytical Chemistry 168 (2023) 117279

Contents lists available at ScienceDirect

Trends in Analytical Chemistry

journal homepage: www.elsevier.com/locate/trac

Recent advances in stimuli-responsive persistent luminescence nanoparticles-based sensors

Xu Zhao [a,b,c], Xue-Mei Gao [d], Tian-Yue Gu [c], Ke-Lin Chen [c], Zhu-Ying Yan [a], Li-Jian Chen [a,b,c], Xiu-Ping Yan [a,b,c,d,*]

[a] State Key Laboratory of Food Science and Resources, Jiangnan University, Wuxi, 214122, China
[b] International Joint Laboratory on Food Safety, Jiangnan University, Wuxi, 214122, China
[c] Institute of Analytical Food Safety, School of Food Science and Technology, Jiangnan University, Wuxi, 214122, China
[d] Key Laboratory of Synthetic and Biological Colloids, Ministry of Education, School of Chemical and Material Engineering, Jiangnan University, Wuxi, 214122, China

ARTICLE INFO

Keywords:
Persistent luminescence nanoparticles
Responsive
Food analysis
Biosensing
Bioimaging

ABSTRACT

Persistent luminescence nanoparticles (PLNPs) are novel optical nanomaterials with repeatable excitation characteristics, which can store and release energy continuously after cessation of excitation. These features make PLNPs have the advantages of no need for in-situ excitation and background fluorescence-free, and are favored in the field of sensing and imaging. Particularly, PLNPs-based responsive sensors have broad prospects in low-background and high-sensitivity detection. In this review, we summarize the design strategies and research progress of responsive PLNPs-based sensors for food analysis, biosensing and bioimaging. We also discuss and look forward to the challenges and opportunities of responsive PLNPs-based sensing systems to promote the development of highly sensitive detection technologies.

1. Introduction

Persistent luminescence nanoparticles (PLNPs) are a new type of optical nanomaterials that can store excitation energy and continuously release energy after the stoppage of the excitation [1–4]. PLNPs-based sensors, therefore, can rely on their own afterglow luminescence for detection without external excitation, which can effectively avoid background fluorescence interference and achieve high signal-to-noise ratio (SNR) detection [5–7]. In addition, the afterglow of PLNPs can be repeatedly excited, the surface is easy to be chemically modified and has good biocompatibility, which makes them meet the needs of different fields [8]. Undoubtedly, PLNPs-based sensors have attracted more and more interest and are widely used in food analysis [9], biosensing [10–12], bioimaging [13,14]. However, conventional always on PLNPs-based sensors are limited by inherent disadvantages, such as lack of specificity, and false positive signal interference from the signal of PLNPs themselves, which hinder the further application of PLNPs-based sensors [15].

Responsive PLNPs-based sensors have the ability of specific recognition of the targets with the targets-mediated signal changes after the surface functionalization of PLNPs, achieving more accurate analysis of targets. Up to now, there are two main response strategies for building responsive PLNPs-based sensors. One kind is based on the targets. For example, the target specific aptamer was selected to modify the PLNPs to achieve the specific recognization [16]. Another strategy is to use variations in the microenvironment of the lesion site to achieve an intelligent diagnosis of related diseases. The microenvironment includes, but is not limited to, weak acidity, overexpression of biomolecules, and increased reactive oxygen species (ROS) production [17,18].

Responsive PLNPs-based sensors are sensitive to physiological, pathological or external stimulation and are considered to be promising next-generation precision detection platforms. To date, this kind of sensor has enabled the detection of food contaminants with a wide linear range and low detection limits [19,20], *in vitro* detection of disease biomarkers with high sensitivity [21], and *in vivo* targeted imaging and diagnosis with high SNR [22,23].

In recent years, several outstanding reviews on the application of PLNPs have been published [24–27]. For example, Yan's group [24] systematically summarized their work on PLNPs-based nanoprobes for biosensing and bioimaging. Zhao and co-workers [25] provided a systematic summary of fluorescence-free detection and sensing based on PLNPs in complex matrices. However, it is difficult to find a

* Corresponding author. State Key Laboratory of Food Science and Resources, Jiangnan University, Wuxi, 214122, China.
E-mail address: xpyan@jiangnan.edu.cn (X.-P. Yan).

https://doi.org/10.1016/j.trac.2023.117279
Received 3 July 2023; Received in revised form 3 September 2023; Accepted 9 September 2023
Available online 17 September 2023
0165-9936/

comprehensive review based on responsive PLNPs-based nanoprobes. Hence, this review details the construction strategies and research progress of responsive PLNPs-based nanoprobes, focusing on the application in food analysis, biosensing and *in vivo* imaging. The challenges and opportunities of responsive PLNPs-based nanoprobes are further discussed.

2. Food contaminants analysis

Food contaminants have caused serious harm to human health and have become a major topic of global concern. It has been reported that three quarters of the 150 million cases of diarrhea worldwide each year are attributed to contaminated food [28]. Heavy metal ions and mycotoxins are important sources of food contamination. The conventional detection methods for these pollutants mainly include enzyme-linked immunosorbent assay, chromatographic analysis, and supercritical fluid extraction and so on [29,30]. These methods require complex sample pretreatment, high requirements for testing instruments and operators, expensive costs, and have low detection sensitivity. Therefore, it is particularly important to develop novel detection methods with high sensitivity, low detection limits and simple operation for food contamination. The unique in situ excitation-free property of PLNPs enable them to effectively avoid the interference of food biological matrix and environmental background, and show a good prospect in the accurate detection of food contaminants. In particular, PLNPs-based responsive sensors have been widely used in food analysis due to their advantages of rapid response, high sensitivity and strong specificity [19,20].

2.1. Heavy metal ions detection

With the development of technology and industry, heavy metal ions are widely found in soil and water, which not only pollute the environment, but also seriously endanger human health. Heavy metal ion can cause irreversible damage to several organs such as the kidney and liver [31,32]. Therefore, rapid and sensitive detection of heavy metal ions is of great significance. There have been many studies on heavy metal detection. For example, Chen et al. [33] constructed a sensor for the quantitative analysis of As(III) using green-light-emitting Zn_2GeO_4:Mn (ZGO:Mn) as an energy emitter. The developed sensor realized the detection of As(III) in drinking water and scallop meat at low concentrations. Qi [19] and co-workers reported a nanobeacon based on a single target response for the detection of the metal ion Pb^{2+} in environmental water samples (Fig. 1). Zn_2GeO_4:Mn nanorods were functionalized with 17E DNA coenzyme, while the other end of the 17E DNA was linked by base complementary pairing to a complementary strand modified with a black hole quencher (BHQ1-sDNA). The black hole quencher BHQ1 strong absorption at 480–580 nm with a high extinction coefficient [34], thus it can quench the luminescence of Zn_2GeO_4:Mn. When Pb^{2+} was found in the sample, the metal-specific DNAzyme was activated and the substrate chains with quenching groups was cleaved. Meanwhile the quencher BHQ1 was separated from the nanobeacon, which lead to the recovery of luminescence of the nanorods, thus realizing the sensitive detection of Pb^{2+}. For another example, Tan's team [35,36] developed a PLNP-based switch sensor based on luminescent resonance energy transfer (FRET) for the detection of Cd^{2+} in real water samples. Cd^{2+} aptamer-modified PLNPs acted as energy donors and BHQ1 attached to the complementary strand cDNA of the aptamer acted as energy acceptors. The aptamer sensor showed a good linear for Cd^{2+} in the range of 0.5–50 μg L^{-1} with a detection limit of 0.35 μg L^{-1}.

Similar to FRET, the internal filter effect (IFE) is a luminescence quenching phenomenon caused by the overlapping of the absorption spectrum of quencher and the emission spectrum of luminescence donor [37,38]. The difference is that IFE requires more flexibility in the distance between quencher and luminescence donor, and the luminescence lifetime of donor will not be attenuated. Wang and colleagues [39]

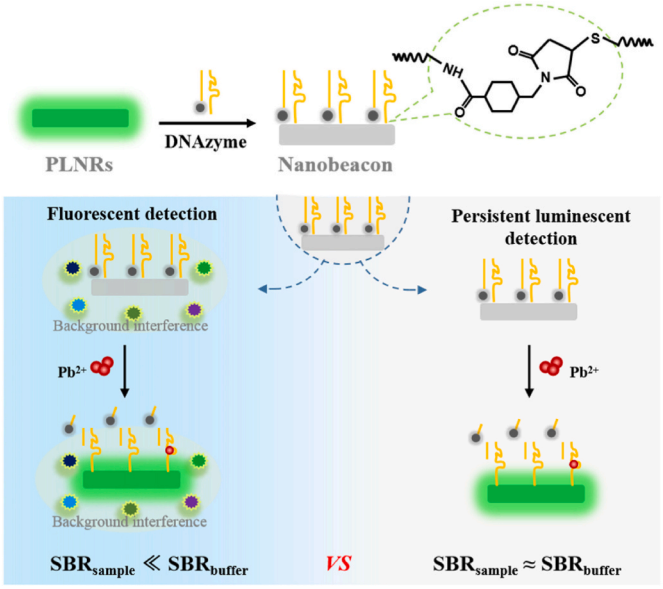

Fig. 1. Schematic illustration of the design of persistent luminescent nanobeacon for the detection of Pb^{2+}. Reproduced from Ref. [19]. Copyright (2022), with permission from Elsevier.

prepared for the first time a PLNPs-based probes based on IFE for As^{3+} detection in complex water samples (Fig. 2). First, ZGGO with good optical properties was employed as an energy donor, and AuNPs overlapping well with the emission of PLNPs were acted as an acceptor. Then, polyethyleneimine (PEI)-functionalized positively charged ZGGO-PEI and dithiothreitol-coated negatively charged gold nanorods (DTT-AuNPs) were obtained and further constructed the IFE-based nanoprobe via electrostatic assembly. When the target As^{3+} was present, it would disrupt the surface electronegativity of AuNPs by binding to DTT, causing the separation of ZGGO and AuNPs and luminescence recovery of the probe at 695 nm. The detection range of the nanoprobe for As^{3+} is 0.067–13.4 μmol L^{-1} with a wide linear range and good results for promising applications.

2.2. Mycotoxin detection

PLNPs-based sensors not only perform well in metal ion detection, but also show convincing applications for fungal toxins. Fungi toxins are toxic secondary metabolites produced and released by fungi during their growth and are widely distributed in food grains and their products. Fungi toxins can produce significant toxicity even at low doses, causing not only genetic mutations, tissue lesions and cancer, but also inevitable damage to kidney and immune system, which seriously endangers human life and health. Therefore, accurate and sensitive detection of mycotoxins in food samples is of great importance.

Jiang [20] reported a aptamer sensor based on FRET for the selective detection of ochratoxin A (OTA) in beer samples. The aptamer sensor exhibited a sensitive response to OTA over a wide linear range of 0.01–10 ng mL^{-1}. Accurate determination combined with efficient removal of hazards from food have more application value. With this

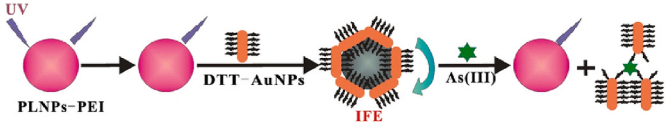

Fig. 2. Schematic illustration of the design of the PLNPs-AuNPs nanoprobe for the detection of As(III) based on IFE. Reproduced from Ref. [39]. Copyright (2019), with permission from Springer Nature.

aim, Yan's group [40] further reported an autofluorescence-free PLNP-based aptamer sensor for the detection and separation of kanamycin in food samples (Fig. 3). Magnetic nanoparticles (MNPs) were selected as energy receptors and separation units, and kanamycin aptamers were attached to their surfaces. Near-infrared emitting $ZnGa_2O_4$: Cr PLNPs were chosen as the energy donor and signal unit, and the complementary strand (cDNA) was functionalized on their surface using a cross-linking agent. The phosphorescent quenching aptamer sensor (MNPs-apt@PLNPs-cDNA) was further constructed through the base complementary pairing. In the presence of kanamycin, the aptamer preferentially bound to kanamycin, resulting in the separation of PLNPs from MNPs and the recovery of phosphorescence. The detection limit was as low as 0.32 pg mL^{-1} and the recovery in milk, honey and milk powder samples were 95.4–106.3%, showing good application prospects.

Accurate detection of a single toxin is very important. However, mycotoxins are diverse, widely distributed, toxic, and widely co-occurring, and the synergistic effects of different mycotoxins will cause greater harm to human beings [41–44]. Therefore, it is of great significance to build a novel method that can detect multiple toxins simultaneously to ensure food safety. To realize highly sensitive synchronous detection of aflatoxin B_1 (AFB_1) and zallalenone (ZEN) in food samples, Yan et al. [45] further designed a PLNPs-based dual-color sensor (Fig. 4). The signal units of $Zn_2GeO_4:Mn^{2+}$ (ZGO:Mn) and $Zn_{1.25}Ga_{1.5}Ge_{0.25}O_4:Cr^{3+}$, Yb^{3+}, Er^{3+} (ZGGO:Cr) with emission wavelengths of 537 nm and 701 nm were functionalized with AFB_1 and ZEN aptamers, respectively. Meanwhlie, magnetic spheres were selected as signal receptors, and complementary strand cDNAs of the two aptamers were grafted on the surface. Finally, the dual-color sensor with quenching phosphorescence was constructed by complementary base hybridization. The sensor has a wide detection range of 0.001–50 ng mL^{-1} for AFB_1 and ZEN with detection limits as low as 0.29 and 0.22 pg mL^{-1}, respectively. The as-prepared sensor shows excellent detection effect and provides a new idea for the simultaneous detection of multiple contaminants.

PLNPs-based sensors can achieve the low background detection of targets. However, the luminescence signals of PLNPs are susceptible to interference from external factors such as temperature, time, probe concentration and instrument parameters, which affect the accuracy of detection [46]. How to eliminate the interference from external factors and build a more intelligent and accurate detection platform is a research hotspot in the development of PLNPs-based sensors. Guo [47] reported a PLNPs-based dual-wavelength ratiometric sensor for sensitive detection of OTA by introducing a reference signal to eliminate the interference of external factors (Fig. 5). Zn_2GeO_4:Mn (ZGM) and $ZnGa_2O_4$:Cr (ZGC) with emission wavelengths of 537 nm and 700 nm were used as a detection probe and a reference probe, respectively. The dual-wavelength ratiometric sensor was further constructed by combining aptamer and BHQ1 quencher-modified cDNA functionalized ZGM and quaternary ammonium salt modified ZGC through electrostatic interaction. The phosphorescence signal ratio change $\Delta(I_{537}/I_{700})$ was linearly related to the concentration of OTA. By introducing reference signal, the sensor effectively eliminates external interference, shows high specificity, and realizes the accurate response of OTA in grain.

Although the luminescence ratiometric detection can be realized by using two kinds of PLNPs, the preparation was complicated and the stability was poor. The development of a simple method to prepare dual-emissive PLNPs and further construction of sensors for ratio detection will be more valuable. For this purpose, Pan [48] designed and constructed a ratiometric luminescent aptasensor based on dual-emissive PLNPs for trace detection of AFB_1 in complex food samples (Fig. 6). $ZnGa_2O_4:Cr_{0.0001}$ (ZGC) with dual-emissive signals at 714 nm and 508 nm was firstly prepared by adjusting the doping amount of Cr^{3+}, the unique luminescence center. The ratiometric luminescent aptasensor was further fabricated by aptamer and Cy5.5-modified cDNA modification. The sensor had a good response to AFB_1 in a wide detection range of 0.05–70 ng mL^{-1}, with low detection limit (0.016 ng mL^{-1}). Compared with the ratiometric sensor based on two PLNPs, the preparation of the sensor based on a single PLNPs was simpler and more convenient, the concentration of the reference signal did not need to be adjusted and optimized, and the ratio relationship between the reference signal and the response signal was more stable and controllable. Therefore, the dual-emissive PLNPs-based ratiometric sensor has more application prospects.

3. Disease marker sensing

Quantitative detection of disease-related chemicals in human blood, body fluids or tissues is one of the important methods of disease diagnosis [49]. Sensitive and accurate sensors are the core of quantitative detection. However, due to the complex composition of biological samples, the interference of autofluorescence or light scattering from biological matrices is unavoidable in real-time detection. PLNPs, which can eliminate the interference of background fluorescence, have shown excellent advantages in the field of biosensing and have received widespread attention.

3.1. Single target detection

The PLNPs-based responsive sensors can be used to achieve sensitive disease detection through the different responses of long afterglow luminescence signals to disease markers. For example, Liu et al. [50] used naked $ZnGa_2O_4:Cr^{3+}$ as a detection probe and achieved detection of hemoglobin (Hb) using a dynamic quenching process induced by Hb to burst the phosphorescence. Li et al. [51] modified Zn_2GeO_4:Mn with

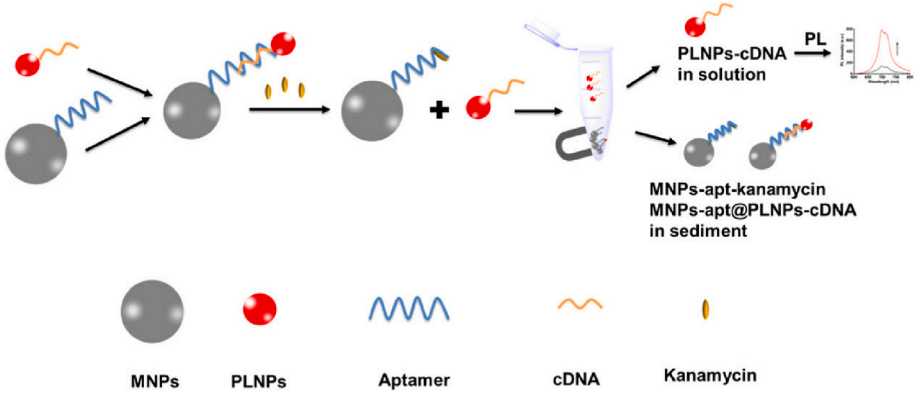

Fig. 3. Illustration of the design and application of MNPs-apt@PLNPs-cDNA aptasensor for kanamycin. Reproduced from Ref. [40]. Copyright (2021), with permission from American Chemical Society.

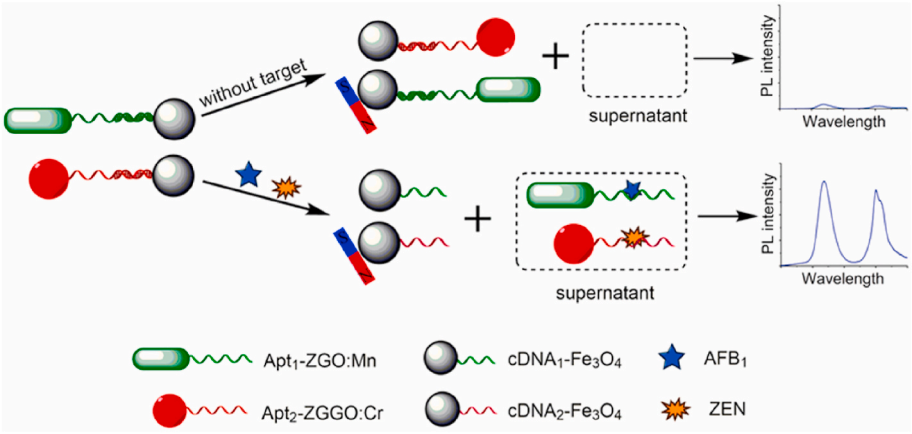

Fig. 4. Illustration of the design and application of the dual-color PLNPs based sensor for simultaneous detection of ZEN and AFB1. Reproduced from Ref. [45]. Copyright (2021), with permission from Elsevier. (For interpretation of the references to colour in this figure legend, the reader is referred to the Web version of this article.)

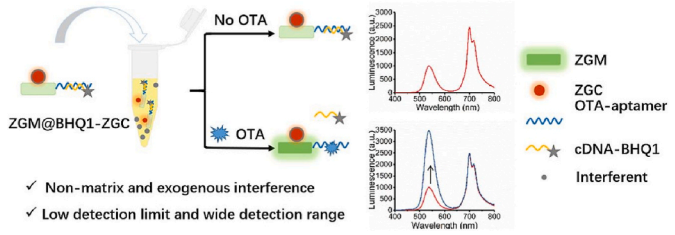

Fig. 5. Illustration of the design and application of the dual-colored PLNPs-based ratiometric aptasensor ZGM@BHQ1-ZGC for the detection of OTA. Reproduced from Ref. [47]. Copyright (2023), with permission from Elsevier.

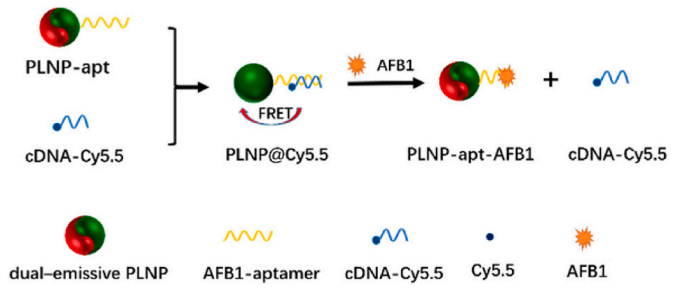

Fig. 6. Illustration for the as-prepared PLNP@Cy5.5 ratiometric aptasensor for the detection of AFB1. Reproduced from Ref. [48]. Copyright (2022), with permission from American Chemical Society.

polydopamine, which has outstanding photothermal properties, to promote the collision process between the signal donor and human serum albumin and further improve the detection sensitivity.

Compared with bare PLNPs, surface modification of PLNPs can improve their specific recognition ability to targets and improve their biocompatibility, which is conducive to the construction of more flexible PLNPs-based sensors. For example, Zhang et al. [52] developed a nanoprobe for the detection of prostate-specific antigen (PSA) in serum based on functionalized PLNPs and Au@Ag@SiO_2 nanoparticles. The sensor has a wide linear range and low detection limit, showing excellent sensitivity and accuracy for PSA. Li et al. [53] demonstrated a nanoprobe for the detection and bioimaging of ascorbic acid (AA) in living cells and in vivo, based on the cobalt oxyhydroxide and $Sr_2MgSi_2O_7$:Eu,Dy PLNPs. The probe can achieve the detection of AA in cells and in vivo without continuous external light excitation. Moreover, Chen [54,55] presented a Zn_2GeO_4:Mn@Fe^{3+} (ZGO:Mn@Fe^{3+}) nanoprobe based on an electron transfer strategy for real-time monitoring of Fe(III) respiratory metabolism. When Fe^{3+} accepted electrons from dynamic Fe(III) respiratory metabolism, the burst sustained luminescence of Zn_2GeO_4:Mn@Fe^{3+} was restored, which enables real-time and dynamic monitoring of microbial metabolis.

Signal amplification is one of the development directions of biosensing, which is helpful to improve sensitivity and accuracy. Tang et al. [56] reported a pH-responsive autofluorescence-free amplified signal biosensor for the bioassay of PSA (Fig. 7).

Zn_2GeO_4: Mn^{2+},Pr^{3+} (ZGOMP), which was degradable under acidic conditions, was used as a detect probe and gluconic acid were employed as a potential trigger agent. Magnetic beads (MB) were modified with anchor DNA and the complementary strand of specific DNA and free aptamer. When PSA was present in the system, the aptamer preferentially bound specifically to the PAS and the hybridization chain reaction process was activated, resulting in the successful loading of large amounts of glucose oxidase (GOD) on the surface of MB. Gluconic acid, the catalytic product of GOD, could change the microenvironmental pH, causing the degradation of ZGOMP, accompanied by a decrease in phosphorescence. Thus, the expected signal amplification effect was achieved. The sensor shows good sensitivity with a detection limit of 0.64 pg mL^{-1}.

Aptamers are commonly used components in target detection, but their affinity can be affected by the carrier. The introduction of signal amplification techniques can enhance detection sensitivity. Yuan et al. [57] constructed a phosphorescence-enhanced PLNP-based nanoprobe for the bioassay of microRNA21 (miR21) in urine samples by introducing photonic crystals (PC). The PC was a highly ordered nanostructure that blocks transmitted light and significantly enhances reflected light. Attaching PLNP to PC dramatically enhances the optical signal of PLNP, thereby improving sensitivity and effectively avoiding interference from fluorescence such as proteins in biological samples.

Low concentration of target is a persistent problem in sensing and detection, and pre-enrichment is one of the countermeasures with great development potential. Yao et al. [58] introduced a metal-organic framwork (MOF) as a pre-enriched functional element and combined with PLNPs to build a dopamine (DA) detection system. DA is intimately related to the physiological functions of the central nervous system, and its dysregulation can lead to various diseases such as Parkinson's disease [59]. Ultra-small $ZnGa_2O_4$:Cr (ZGC) PLNPs were attracted to the surface of HZIF-8 MOF by electrostatic effect to offer DA sensor. The multilevel pore structure of HIZIF-8 was also more conducive to the stability of this sensor. Due to the alkaline microenvironment provided by HIZF-8, DA was easily oxidized and aggregated on the surface to generate polydopamine (PDA). While destroying the structure of HIZF-8, PDA acted as

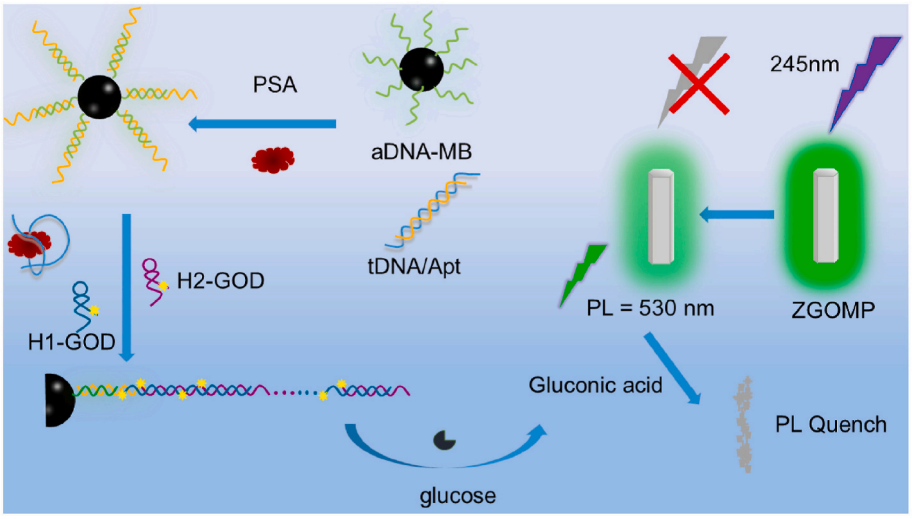

Fig. 7. Schematic illustration of PLNP-based aptasensor for the detection of PSA. (H1: hairpin 1; H2: hairpin 2; aDNA: anchor DNA; tDNA: trigger DNA; Apt: PSA aptamer). Reproduced from Ref. [56]. Copyright (2021), with permission from Elsevier.

an electron acceptor to capture the photoexcited electrons of ZGC, thus quenching the luminescence of PLNPs and realizing highly sensitive detection of DA in the range of 0.0025–75 μM.

3.2. *Multi-target simultaneous detection*

Multiple metrics are required for disease diagnosis, so single-target sensing is not suitable for complex and realistic needs. Yan and colleagues [60] reported a dual-signal detection platform based on functionalized gold nanoparticles (AuNPs) and near-infrared PLNPs (Fig. 8), which can simultaneously detect L-cysteine (L-Cys) and insulin (Ins) for the diagnosis of diabetes. PLNPs modified with Ins aptamer and AuNPs functionalized with complementary chains were synthesized, respectively. When L-Cys was present in the system, the dispersed AuNPs gathered into clusters under the action of van der Waals forces and intermolecular electrostatic interactions, and the absorption peak red-shifted from 520 nm to 660 nm, thus realizing the ratio detection of L-Cys, which was effective in the range of 10 nM-5.5 μM with a limit of detection (LOD) of 2.2 nM. PLNPs with 698 nm phosphorescence emission was then added into the system as a FRET signal donor, and coupled with the aggregated AuNPs, an energy receptor, to form a phosphorescence quenching sensor for Ins. Until the target Ins was competitively bound to the complementary chain and FRET was cut off, the donor receptor was separated, phosphorescence was restored, and

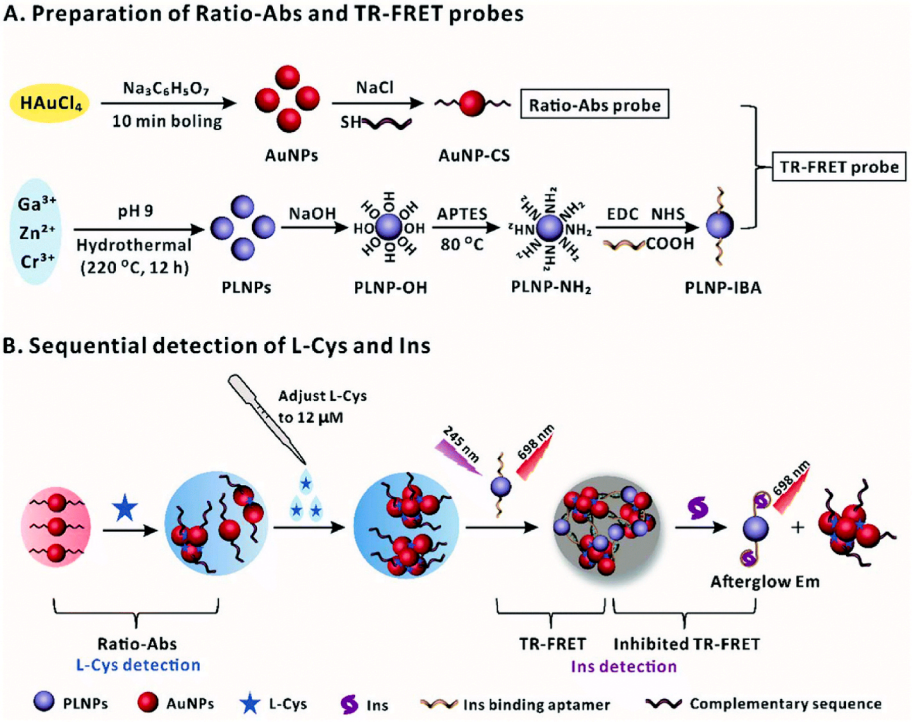

Fig. 8. Schematic illustration of the design and synthesis of dual-signaling sensor for high-sensitive detection of L-Cys and Ins. Complementary sequence represents partial complementary sequence of IBA which represents Ins binding aptamer. Reprinted with permission from Ref. [60]. Copyright (2018), with permission from The Royal Society of Chemistry.

the detection of Ins was achieved in the linear range of 12 ppmol L^{-1} to 3.44 npmol L^{-1}, and the detection limit was as low as 2.06 pmol L^{-1}. The proposed sensor showed excellent precision in detecting Ins in the range of 12 pM to 3.44 nM with LOD of 2.06 pM.

Compared with the sensor based on a single PLNPs, the dual-signal platform constructed based on two kinds of PLNPs of wavelengths have a higher SNR and a broader application prospect [61,62]. For instance, Shi's group [61] developed a dual-target sensor based on two kinds of PLNPs for simultaneous detection of PSA and carcinoembryonic antigen (CEA). Green-emitted Zn_2GeO_4:Mn (ZGO:Mn) and red-emitted $ZnGa_2O_4$:Cr (ZGC), which noninterfering emission wavelengths, were synthesized as phosphorescent emitters, and then PSA and CEA aptamers were modified on the surface respectively. Polydopamine nanoparticles (PDANSs) with broad-spectrum absorption were selected as phosphorescent quenching agents, and ZGO:Mn and ZGC were assembled on their surfaces through π -π stacking between PDANSs and aptamers. Luminescence of ZGO:Mn and ZGC was quenched under the action of FRET and photo-induced electron transfer. When PSA and CEA were present in the system, the aptamer bound preferentially to the target and detached from PDANSs, so the burst system was broken and the luminescence was restored, the quenching system was broken, and phosphorescence was restored, thus realizing the dual-target determination with wide linear range and low LOD.

4. *In vivo* imaging

Bioimaging can monitor various biological processes in their native environment and has proved to be an indispensable tool in modern biological research. Many fluorescent probes have been developed, such as organic dyes, fluorescent proteins and metal complexes [63], however these probes require continuous excitation during bioimaging and cannot avoid the auto-fluorescence interference of tissue. The fluorescence lifetimes of proteins and small molecules in the biological environment are at the nanosecond level [64], while the luminescence lifetime of PLNPs is as long as several hours or even days, which has become an ideal imaging material without tissue auto-fluorescence interference. Currently, PLNPs-based sensors have many applications in imaging, but they are mainly used for drug delivery and the signals are always on [14]. Besides, they are also prone to aggregation in the endothelial reticular system and cannot specifically distinguish lesion sites. Taking into account the characteristics of the microenvironment at the lesion site, responsive PLNPs-based sensors have been designed, which are more suitable for biological imaging applications. Up to now, many works have been published on responsive PLNP-based probes for high sensitivity and selectivity imaging in living systems [65,66]. In this section, we take the bacterial microenvironment as the research object to report the research progress of responsive PLNP-based probes for bacterial infection imaging.

Bacterial infections are one of the common complications after skin trauma, burns, and surgery, which not only severely affect the speed of wound healing, but also greatly increase the risk of death of patients. It is reported that one-third of deaths worldwide are caused by pathogenic bacterial infections [67–69]. With the increase in public health events caused by bacterial infections, accurate biosensing of bacterial infections has become a topic of wide interest for researchers. The microenvironment of infected area was significantly different from that of normal tissue, for example, the pH decreases, the content of certain enzymes secreted by bacteria increases, and the ROS level increases [70]. The change of microenvironment provides the possibility for constructing activated for specific imaging of bacterial infection.

4.1. *Single-factor responsive PLNPs-based probes*

The weak acidity of bacterial infection site is considered as an appropriate internal trigger for developing responsive PLNPs-based sensors to realize accurate imaging of bacterial infection. For example, Wei et al. [71] have constructed a pH-responsive nanoplatform based on acid-degraded PLNPs for bacterial infection imaging (Fig. 9). Zn_2GeO_4:Mn PLNPs was used as an imaging signal unit and a potential chemodynamic therapy reagent, and combined with asymmetric cyanine probe (PS), a photodynamic therapy reagent, to form a therapeutic platform (PLNP-PS). The as-developed PLNP-PS had good stability in normal tissues, but degraded in the weakly acidic microenvironment of bacteria, and the phosphorescence was significantly reduced, so as to achieve bacterial targeted imaging. Meanwhile, Mn^{2+} was released as a Fenton reagent to achieve chemdynamic sterilization. The free PS was protonated, accompanied by charge reversal, and then the targeted binding with bacteria to achieve photodynamic sterilization under the irradiation of 808 nm laser.

4.2. *Multi-factor responsive PLNPs-based probes*

Compared with single-factor response, multi-factor activated probes are more accurate. Wang and others [72] have designed a pH/H_2O_2/-hyaluronidase (HA) multi-factor responsive PLNPs-based probe (Fig. 10) for bacterial-targeted imaging. Mesoporous silica (MSN) shell was coated on the surface $Zn_{1.2}Ga_{1.6}Ge_{0.2}O_4$:$Cr^{3+}$ PLNPs to load the bactericidal drug cinnamic acid (CA). Further modification of HA and MnO_2 shells to obtain the required multifunctional probe. When the nanoprobe reached the weakly acidic infection site, the outermost layer of MnO_2 was reduced to Mn^{2+} by the excess H_2O_2, and the luminescence of PLNPs was restored to achieve accurate in vivo imaging. Meanwhile, HA shell layer was hydrolyzed by the hyaluronidase overexpressed at the bacterial infection site, releasing CA and playing a role of chemical sterilization. In addition, the Fenton reaction triggered by Mn^{2+} achieved a synergistic bactericidal effect.

5. Conclusion and outlook

PLNPs have been widely used in the field of high SNR detection/imaging because of their in-situ excitation-free characteristic. The construction of responsive PLNPs-based sensors can improve the specificity of detection/imaging, eliminate the interference of false positive signals, and show a broader application prospect. This review summarizes in detail the applications of responsive PLNPs-based probes in food analysis, biosensing and imaging with emphasis on the response mechanisms of different sensors. Based on the specific properties of the targets or environment, intelligent responsive platforms are constructed to realize specific recognition of various food contaminants, biomarkers and diseased tissues *in vivo*.

Although a lot of research achievements have been made in the last decade, the development and application of responsive PLNPs-based sensors still face some difficulties and challenges. Firstly, controllable preparation of small-sized and high performance PLNPs. Although many efforts have been made in the preparation of PLNPs, the preparation of PLNPs with controllable size, uniform morphology and excellent optical properties is still a difficult problem to be solved urgently. Second, improvement of the surface functionalization strategy of PLNPs. The functionalization of PLNPs has also been shown to avoid the nontargeted capture and improve the hemocompability [73]. It is urgent to develop new strategies to improve the modification rate and simplify the synthesis steps to obtain better performance. Third, development of intelligent responsive sensors. For example, it is urgent to develop a small-sized intelligent responsive PLNPs-based probe for *in vivo* imaging, so as to reduce the non-targeted aggregation of large-sized PLNPs in the endothelial reticular system such as liver and kidney and realize more accurate biological imaging. Last but not least, expansion the application field. At present, the research of responsive PLNPs-based sensors in the field of biological imaging mainly focuses on bacterial infection and cancer, and it is urgent to develop more PLNPs-based sensors with excellent performance for more fields, such as neurological diseases, diabetes and other life-threatening diseases.

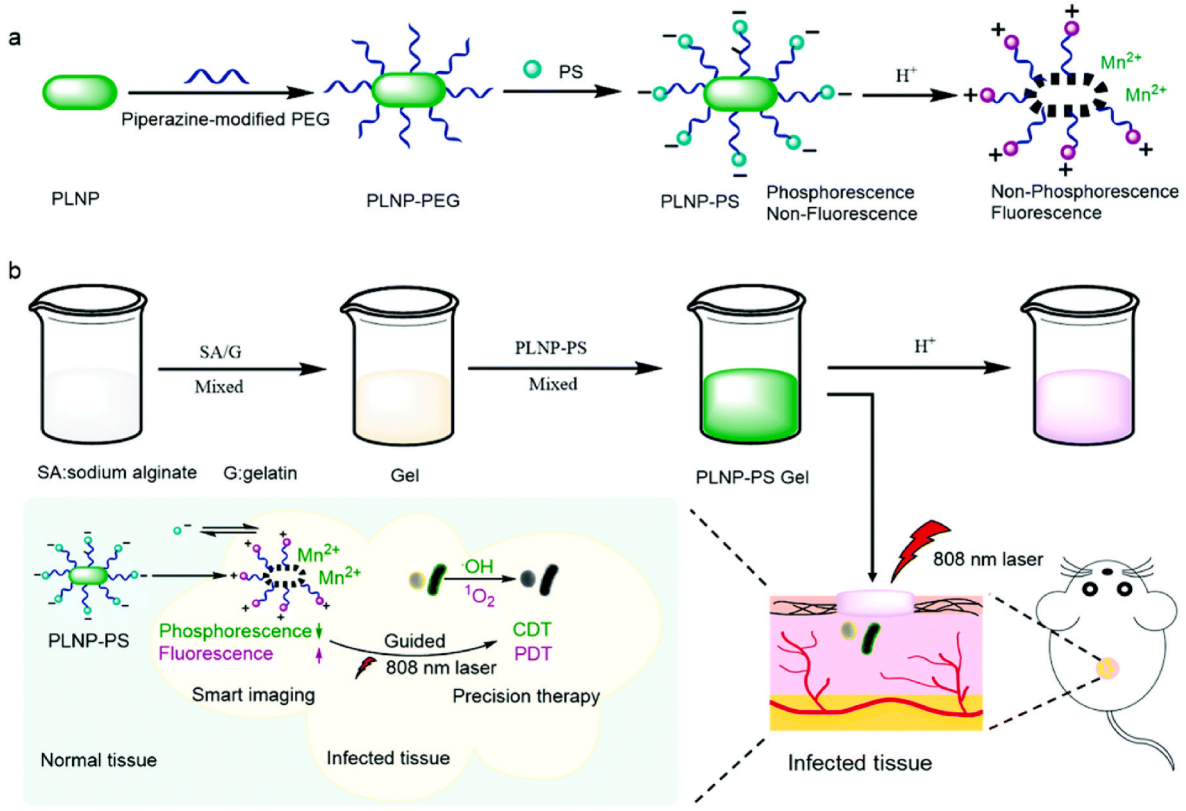

Fig. 9. Schematic illustration of the synthesis and design of the PLNP-PS theranostic platform. (a) Design strategy and synthesis of PLNP-PS. (b) Illustration of the design of PLNP-PS for phosphorescence/fluorescence dual-channel imaging-guided synergistic sterilization. Reprinted with permission from Ref. [71]. Copyright (2022), with permission from The Royal Society of Chemistry.

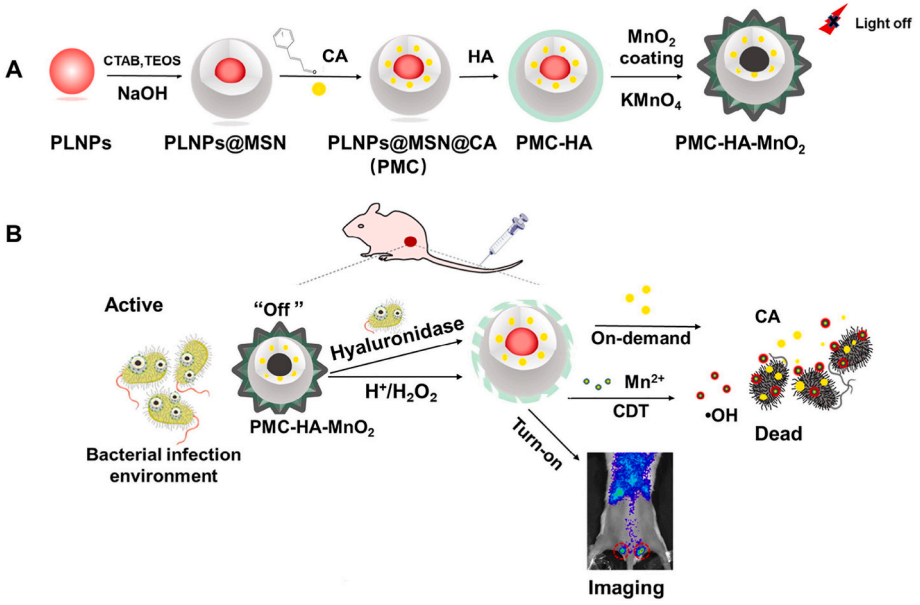

Fig. 10. (a) Illustration for the design of the multifunctional probe. (b) Schematic illustration of the multifunctional probe for bacterial microenvironment-responsive precise imaging and sterilization. Reprinted with permission from Ref. [72]. Copyright (2022), with permission from Elsevier.

Declaration of competing interest

The authors declare that they have no known competing financial interests or personal relationships that could have appeared to influence the work reported in this paper.

Data availability

No data was used for the research described in the article.

Acknowledgements

The authors appreciate the financial supported by the National Natural Science Foundation of China (No. 21934002, 21804056 and 22206060), the Natural Science Foundation of Jiangsu Province, China (No. BK20180581) and the Program of "Collaborative Innovation Center of Food Safety and Quality Control in Jiangsu Province".

References

[1] W.R. Algar, M. Massey, K. Rees, R. Higgins, K.D. Krause, G.H. Darwish, W. J. Peveler, Z. Xiao, H.Y. Tsai, R. Gupta, K. Lix, M.V. Tran, H. Kim, Chem. Rev. 121 (2021) 9243, https://doi.org/10.1021/acs.chemrev.0c01176.
[2] L. Yang, S. Gai, H. Ding, D. Yang, L. Feng, P. Yang, Adv. Opt. Mater. (2023), https://doi.org/10.1002/adom.202202382.
[3] S. Wu, Y. Li, W. Ding, L. Xu, Y. Ma, L. Zhang, Nano-Micro Lett. 12 (2020) 70, https://doi.org/10.1007/s40820-020-0404-8.
[4] V. Rajendran, M.-H. Fang, G.N.D. Guzman, T. Lesniewski, S. Mahlik, M. Grinberg, G. Leniec, S.M. Kaczmarek, Y.-S. Lin, K.-M. Lu, C.-M. Lin, H. Chang, S.-F. Hu, R.-S. Liu, ACS Energy Lett. 3 (2018) 2679, https://doi.org/10.1021/acsenergylett.8b01643.
[5] P. Pei, Y. Chen, C. Sun, Y. Fan, Y. Yang, X. Liu, L. Lu, M. Zhao, H. Zhang, D. Zhao, X. Liu, F. Zhang, Nat. Nanotechnol. 16 (2021) 1011, https://doi.org/10.1038/s41565-021-00922-3.
[6] Q. Miao, C. Xie, X. Zhen, Y. Lyu, H. Duan, X. Liu, J.V. Jokerst, K. Pu, Nat. Biotechnol. 35 (2017) 1102, https://doi.org/10.1038/nbt.3987.
[7] C. Ma, H. Liu, F. Ren, Z. Liu, Q. Sun, C. Zhao, Z. Li, Cryst. Growth Des. 20 (2020) 1859, https://doi.org/10.1021/acs.cgd.9b01575.
[8] Q. Luo, W. Wang, J. Tan, Q. Yuan, Chin. J. Chem. 39 (2021) 1009, https://doi.org/10.1002/cjoc.202000583.
[9] M. Zhang, X. Guo, Trends Food Sci. Technol. 129 (2022) 621, https://doi.org/10.1016/j.tifs.2022.11.013.
[10] S. Hu, Z. Li, Q. Luo, Q. Ma, N. Chen, L. Fu, J. Wang, R. Yang, Q. Yuan, Cryst. Growth Des. 19 (2019) 2322, https://doi.org/10.1021/acs.cgd.9b00012.
[11] C.Y. Li, B. Zheng, L.L. Lu, W.K. Fang, M.Q. Zheng, J.L. Gao, L. Yuheng, D.W. Pang, H.W. Tang, Anal. Chem. 93 (2021), 12514, https://doi.org/10.1021/acs.analchem.1c01403.
[12] J.L. Kong, R. Zou, G.L. Law, Y. Wang, Sci. Adv. 8 (2022), https://doi.org/10.1126/sciadv.abm7077.
[13] N. Liu, X. Chen, X. Sun, X. Sun, J. Shi, J. Nanobiotechnol. 19 (2021) 113, https://doi.org/10.1186/s12951-021-00862-z.
[14] J. Kong, Y. Sun, X. Ge, M. Mao, H. Yu, Y. Wang, Adv. Funct. Mater. 33 (2022), https://doi.org/10.1002/adfm.202209579.
[15] G. Ramirez-Garcia, S. Gutierrez-Granados, M.A. Gallegos-Corona, L. Palma-Tirado, F. d'Orlye, A. Varenne, N. Mignet, C. Richard, M. Martinez-Alfaro, Int. J. Pharm. 532 (2017) 686, https://doi.org/10.1016/j.ijpharm.2017.07.015.
[16] F. Feng, X. Chen, G. Li, S. Liang, Z. Hong, H.F. Wang, ACS Sens. 3 (2018) 1846, https://doi.org/10.1021/acssensors.8b00680.
[17] Y. Li, Z. Chen, L. Gu, Z. Duan, D. Pan, Z. Xu, Q. Gong, Y. Li, H. Zhu, K. Luo, Expet Opin. Drug Deliv. 19 (2022) 337, https://doi.org/10.1080/17425247.2022.2050211.
[18] N.M. Anderson, M.C. Simon, Curr. Biol. 30 (2020) R921, https://doi.org/10.1016/j.cub.2020.06.081.
[19] Q. Luo, L. Qin, P. Zhang, B. Feng, X. Ye, T. Qing, Z. Qing, Anal. Chim. Acta 1198 (2022), 339555, https://doi.org/10.1016/j.aca.2022.339555.
[20] Y.Y. Jiang, X. Zhao, L.J. Chen, C. Yang, X.B. Yin, X.P. Yan, Talanta 218 (2020), 121101, https://doi.org/10.1016/j.talanta.2020.121101.
[21] Z. Pan, D. Yang, J. Lin, K. Shao, S. Shi, Y.J. Teng, H. Liu, Y. She, Anal. Chim. Acta 1194 (2022), 339408, https://doi.org/10.1016/j.aca.2021.339408.
[22] B. Zhang, D. Lu, H. Duan, Biomater. Sci. 11 (2023) 356, https://doi.org/10.1039/d2bm01573k.
[23] Y. Feng, L. Zhang, R. Liu, Y. Lv, Biosens. Bioelectron. 144 (2019), 111671, https://doi.org/10.1016/j.bios.2019.111671.
[24] S.K. Sun, H.F. Wang, X.P. Yan, Acc. Chem. Res. 51 (2018) 1131, https://doi.org/10.1021/acs.accounts.7b00619.
[25] X. Zhao, L.-J. Chen, K.-C. Zhao, Y.-S. Liu, J.-l. Liu, X.-P. Yan, TrAC, Trends Anal. Chem. 118 (2019) 65, https://doi.org/10.1016/j.trac.2019.05.025.
[26] J. Liu, T. Lecuyer, J. Seguin, N. Mignet, D. Scherman, B. Viana, C. Richard, Adv. Drug Deliv. Rev. 138 (2019) 193, https://doi.org/10.1016/j.addr.2018.10.015.
[27] K. Huang, N. Le, J.S. Wang, L. Huang, L. Zeng, W.C. Xu, Z. Li, Y. Li, G. Han, Adv. Mater. 34 (2022), e2107962, https://doi.org/10.1002/adma.202107962.
[28] V.S. Manikandan, B. Adhikari, A. Chen, Analyst 143 (2018) 4537, https://doi.org/10.1039/C8AN00497H.
[29] F. Sharmin, B.G. Jeong, J. Jung, V. Quines, J. Chun, J. Food Sci. Technol. 54 (2017) 1837, https://doi.org/10.1007/s13197-017-2615-7.
[30] G. Alvarez-Rivera, M. Bueno, D. Ballesteros-Vivas, A. Cifuentes, TrAC, Trends Anal. Chem. 123 (2020), https://doi.org/10.1016/j.trac.2019.115761.
[31] L. Li, Y. Zhang, J.A. Ippolito, W. Xing, K. Qiu, H. Yang, Environ. Pollut. 257 (2020), 113641, https://doi.org/10.1016/j.envpol.2019.113641.
[32] J.Y. Yang, T. Yang, X.Y. Wang, M.L. Chen, Y.L. Yu, J.H. Wang, Anal. Chem. 90 (2018) 6945, https://doi.org/10.1021/acs.analchem.8b01222.
[33] T. Chen, H.T. Wang, Z.P. Wang, M.Q. Tan, Nanomaterials 10 (2020), https://doi.org/10.3390/nano10030551.
[34] Y. Li, L. Sun, Q. Zhao, Anal. Bioanal. Chem. 410 (2018) 6269, https://doi.org/10.1007/s00216-018-1237-x.
[35] B. Lai, R. Wang, X. Yu, H. Wang, Z. Wang, M. Tan, Foods 9 (2020), https://doi.org/10.3390/foods9121758.
[36] B. Lai, H. Wang, W. Su, Z. Wang, B.-W. Zhu, C. Yu, M. Tan, Talanta 232 (2021), https://doi.org/10.1016/j.talanta.2021.122409.
[37] Y. Li, J. Cai, F. Liu, H. Yu, F. Lin, H. Yang, Y. Lin, S. Li, Mikrochim. Acta 185 (2018) 134, https://doi.org/10.1007/s00604-017-2655-8.
[38] F. Zu, F. Yan, Z. Bai, J. Xu, Y. Wang, Y. Huang, X. Zhou, Microchim. Acta 184 (2017) 1899, https://doi.org/10.1007/s00604-017-2318-9.
[39] K. Ge, J. Liu, P. Wang, G. Fang, D. Zhang, S. Wang, Microchim. Acta 186 (2019) 197, https://doi.org/10.1007/s00604-019-3294-z.
[40] B.B. Wang, X. Zhao, L.J. Chen, C. Yang, X.P. Yan, Anal. Chem. 93 (2021) 2589, https://doi.org/10.1021/acs.analchem.0c04648.
[41] H.J. Lee, D. Ryu, J. Agric. Food Chem. 65 (2017) 7034, https://doi.org/10.1021/acs.jafc.6b04847.
[42] C. Gruber-Dorninger, T. Jenkins, G. Schatzmayr, Toxins 11 (2019), https://doi.org/10.3390/toxins11070375.
[43] M. Kumar, G. Singh, N. Kaur, N. Singh, ACS Appl. Mater. Interfaces 14 (2022) 910, https://doi.org/10.1021/acsami.1c19744.
[44] X. Wang, Y. Zhao, X. Qi, T. Zhao, X. Wang, F. Ma, L. Zhang, Q. Zhang, P. Li, J. Hazard Mater. 431 (2022), 128531, https://doi.org/10.1016/j.jhazmat.2022.128531.
[45] Y.Y. Jiang, X. Zhao, L.J. Chen, C. Yang, X.B. Yin, X.P. Yan, Talanta 232 (2021), 122395, https://doi.org/10.1016/j.talanta.2021.122395.
[46] L. Wang, Z. Shang, M. Shi, P. Cao, B. Yang, J. Zou, RSC Adv. 10 (2020), 11418, https://doi.org/10.1039/D0RA00628A.
[47] J.X. Guo, L.M. Pan, M.C. Wang, L.J. Chen, X. Zhao, Food Chem. 413 (2023), 135611, https://doi.org/10.1016/j.foodchem.2023.135611.
[48] L.M. Pan, X. Zhao, X. Wei, L.J. Chen, C. Wang, X.P. Yan, Anal. Chem. 94 (2022) 6387, https://doi.org/10.1021/acs.analchem.2c00861.
[49] J. Rasmussen, H. Langerman, Degener. Neurol. Neuromuscul. Dis. 9 (2019) 123, https://doi.org/10.2147/DNND.S228939.
[50] Y. Liu, Y. Wang, K. Jiang, S. Sun, S. Qian, Q. Wu, H. Lin, Talanta 206 (2020), 120206, https://doi.org/10.1016/j.talanta.2019.120206.
[51] L. Gao, X. Zhang, R. Yang, Z. Lv, W. Yang, Y. Hu, B. Zhou, Microchim. Acta 188 (2021) 429, https://doi.org/10.1007/s00604-021-05097-1.
[52] Y. Zhao, F. Zheng, L. Shi, H. Liu, W. Ke, ACS Appl. Mater. Interfaces 11 (2019), 40669, https://doi.org/10.1021/acsami.9b14901.
[53] N. Li, Y. Li, Y. Han, W. Pan, T. Zhang, B. Tang, Anal. Chem. 86 (2014) 3924, https://doi.org/10.1021/ac5000587.
[54] N. Chen, N. Du, W. Wang, T. Liu, Q. Yuan, Y. Yang, Angew. Chem. 61 (2022), e202115572, https://doi.org/10.1002/ange.202115572.
[55] N. Chen, D. Cheng, T. He, Q. Yuan, Chin. J. Chem. 41 (2023) 1836, https://doi.org/10.1002/cjoc.202200839.
[56] Z. Yin, L. Zhu, Z. Lv, M. Li, D. Tang, Talanta 233 (2021), 122563, https://doi.org/10.1016/j.talanta.2021.122563.
[57] Y. Wang, Z. Li, Q. Lin, Y. Wei, J. Wang, Y. Li, R. Yang, Q. Yuan, ACS Sens. 4 (2019) 2124, https://doi.org/10.1021/acssensors.9b00927.
[58] T. Yao, G. Dong, S. Qian, Y. Cui, X. Chen, T. Tan, L. Li, Sens. Actuators, B 357 (2022), https://doi.org/10.1016/j.snb.2022.131470.
[59] B. Channer, S.M. Matt, E.A. Nickoloff-Bybel, V. Pappa, Y. Agarwal, J. Wickman, P. J. Gaskill, Pharmacol. Rev. 75 (2023) 62, https://doi.org/10.1124/pharmrev.122.000618.
[60] J. Li, C. Yang, W.L. Wang, X.P. Yan, Nanoscale 10 (2018), 14931, https://doi.org/10.1039/c8nr04414g.
[61] L. Shi, J. Shao, X. Jing, W. Zheng, H. Liu, Y. Zhao, ACS Sustainable Chem. Eng. 8 (2020) 686, https://doi.org/10.1021/acssuschemeng.9b06621.
[62] L. Shi, W. Zheng, H. Miao, H. Liu, X. Jing, Y. Zhao, Microchim. Acta 187 (2020) 615, https://doi.org/10.1007/s00604-020-04593-0.
[63] S.S. Xue, Y. Li, W. Pan, N. Li, B. Tang, Chem. Commun. 59 (2023) 3040, https://doi.org/10.1039/D2CC07008A.
[64] Q. Lin, Z. Li, Q. Yuan, Chin. Chem. Lett. 30 (2019) 1547, https://doi.org/10.1016/j.cclet.2019.06.016.
[65] R. Zou, J. Li, T. Yang, Y. Zhang, J. Jiao, K.L. Wong, J. Wang, Theranostics 11 (2021) 8448, https://doi.org/10.7150/thno.59840.
[66] Z. Zhang, H. Yan, B. Qiu, P. Ran, W. Cao, X. Jia, K. Huang, X. Li, Small 18 (2022), e2200813, https://doi.org/10.1002/smll.202200813.
[67] L.X. Yan, L.J. Chen, X. Zhao, X.P. Yan, Adv. Funct. Mater. 30 (2020), https://doi.org/10.1002/adfm.201909042.
[68] J. Huo, Q. Jia, H. Huang, J. Zhang, P. Li, X. Dong, W. Huang, Chem. Soc. Rev. 50 (2021) 8762, https://doi.org/10.1039/d1cs00074h.
[69] B. Jia, X. Du, W. Wang, Y. Qu, X. Liu, M. Zhao, W. Li, Y.Q. Li, Adv. Sci. 9 (2022), e2105252, https://doi.org/10.1002/advs.202105252.
[70] Y. Zhong, X.T. Zheng, S. Zhao, X. Su, X.J. Loh, ACS Nano 16 (2022), 19840, https://doi.org/10.1021/acsnano.2c08262.
[71] X. Zhao, X. Wei, L.J. Chen, X.P. Yan, Biomater. Sci. 10 (2022) 2907, https://doi.org/10.1039/d2bm00374k.
[72] B.B. Wang, L.X. Yan, L.J. Chen, X. Zhao, X.P. Yan, J. Colloid Interface Sci. 610 (2022) 687, https://doi.org/10.1016/j.jcis.2021.11.125.
[73] T. Lecuyer, N. Bia, P. Burckel, C. Loubat, A. Graillot, J. Seguin, Y. Corvis, J. Liu, L. Valero, D. Scherman, N. Mignet, C. Richard, Nanoscale 14 (2022) 1386, https://doi.org/10.1039/D1NR07114A.